telecom

MDPI

Article

Adaptive Power Control for Cooperative Covert Communications with Imperfect CSI

Ling Yang [1], Wenhao Li [1], Liang Tang [2,*], Zhengyun He [1], Junfeng He [1], Yunhui Liu [1], Zhusong Su [1] and Yanzhe Tan [1]

[1] The School of Transportation and Electrical Engineering, Hunan University of Technology, Zhuzhou 412007, China; lingyang0523@126.com (L.Y.); liwh18774190132@163.com (W.L.); zhengyun_he@126.com (Z.H.); 15973817069@163.com (J.H.); liuyunhui1216@126.com (Y.L.); m15773868831@163.com (Z.S.); 18684713267@163.com (Y.T.)

[2] The College of Science, Hunan University of Technology, Zhuzhou 412007, China

* Correspondence: tangliang082@126.com

Abstract

To address the issue that transmitters in existing decode-and-forward (DF) cooperative covert communications hardly acquire all the required channel state information (CSI), this study proceeds as follows. First, an adaptive power strategy for cooperative covert communications based on partial CSI is proposed. Second, the closed-form analytical expression of the covert constraint is derived using the Kullback–Leibler (KL) divergence. Finally, an optimization problem is formulated with the objective of maximizing the covert transmission rate, and the optimal selection of power control parameters is derived. The numerical results demonstrate that in cooperative covert communications, the adaptive power strategy significantly enhances the system's covert transmission rate compared to the constant power strategy, particularly under relaxed covert constraints. Meanwhile, the proposed strategy also markedly reduces the transmission outage probability. Overall comparative analysis confirms that the adaptive power strategy effectively improves the comprehensive covert performance of the system.

Keywords: covert communication; adaptive power control; partial channel state information; cooperative communication; decode-and-forward relay

1. Introduction

In wireless covert communication, traditional encryption and physical-layer security techniques primarily ensure the confidentiality of information content but struggle to conceal the very existence of the communication behavior itself [1–3]. An adversarial monitor can detect communication links through signal detection and localization techniques, thereby launching jamming or attacks [4,5]. Consequently, covert communication technology has emerged, which fundamentally aims to keep the warden from reliably ascertaining whether the source node and its destination are actively exchanging information, thus hiding the very existence of the transmission [6]. This technology plays a crucial role in scenarios such as military reconnaissance and privacy protection [7–9].

Power control is one of the key technologies in covert communication. By dynamically adjusting the transmit power of the source or a jammer, it not only adapts to channel fading to ensure transmission reliability but also introduces uncertainty into the signal received by the monitor, thereby enhancing covertness. Research following this technical path has been extensively conducted by scholars, addressing various system architectures and practical

Check for updates

Academic Editor: Hector E. Nistazakis

Received: 3 June 2026
Revised: 6 July 2026
Accepted: 30 July 2026
Published: 1 October 2026

Copyright: © 2026 by the authors. Licensee MDPI, Basel, Switzerland. This article is an open access article distributed under the terms and conditions of the Creative Commons Attribution (CC BY) license.

constraints. Specifically, Reference [10] proposed a channel inversion power control scheme for downlink non-orthogonal multiple access (NOMA) systems. Building on this, the jammer-aided scenario with imperfect channel state information (CSI) was examined in [11], where an adaptive power adjustment framework was put forward. Reference [12] extended the research to scenarios involving multiple jammers. A comparative study between standard and truncated channel-inversion policies was provided in [13]. References [14–16] deepened and expanded the research on power control strategies in scenarios such as full-duplex relaying, device-to-device cellular networks, and uplink NOMA, respectively. Despite these advances, most existing power control schemes rely on the availability of full CSI, which is often impractical in dynamic environments.

When only partial channel state information is available, power control becomes considerably more challenging. To tackle this issue, a joint optimization framework for jammer selection and power allocation was developed in [17]. Reference [18] focused specifically on the power control optimization problem in finite block length scenarios. With the emergence of new scenarios such as intelligent reflecting surfaces (IRS), Reference [19] investigated the issue of excessive channel estimation overhead in distributed IRS. Furthermore, Reference [20] investigates covert communications with only partial CSI under active reconfigurable intelligent surfaces. However, these works primarily focus on single-hop or static relaying scenarios and do not address the unique challenges introduced by multi-hop DF relay systems with partial CSI.

To extend communication coverage and enhance link reliability, cooperative communication technology has attracted widespread attention. In the context of DF relaying, ref. [21] examined a multi-antenna setup and put forward two transmission strategies—random beamforming and maximum-ratio transmission. Reference [22] explored multi-antenna and device-to-device (D2D) covert communication assisted by DF relays. Furthermore, Reference [23] provided a comprehensive analysis of mode selection and power control for both full-duplex and half-duplex DF relays. Nevertheless, these studies assume that the relay has access to perfect CSI, which is a strong assumption that limits their applicability in practical systems where CSI uncertainty is inevitable.

Research gap and motivation: Although the aforementioned studies have made significant progress in power control, partial CSI adaptation, and DF relay design, a critical issue remains underexplored: most existing DF relay schemes assume that the relay can obtain perfect CSI, failing to deeply integrate adaptive power control with the multi-link CSI uncertainty inherent in DF relaying systems. In view of this, we study DF relay-assisted covert communication with partial CSI and propose an adaptive power control framework that jointly regulates the source and relay transmit powers. The primary contributions are outlined below.

(1) We consider an adaptive power control strategy for cooperative covert systems that operate with partial CSI. This strategy dynamically adjusts the transmit power of both the source and the relay under unknown channel conditions, leverages a Kullback–Leibler (KL) divergence constraint to satisfy the covertness requirement, ensures interruption-free two-hop transmission, and ultimately establishes a dynamic power regulation mechanism suitable for partial CSI environments.
(2) We formulate the system optimization problem by incorporating the DF relay protocol and the partial-CSI power adaptation rule, derive the closed-form covertness constraint, and obtain the end-to-end covert throughput and overall outage probability.
(3) The proposed scheme fully leverages the advantages of adaptive power control in partial CSI. Under stringent covertness constraints, both schemes exhibit comparable performance. However, when the constraints are relaxed, the adaptive strategy, through dynamic power adjustment, can more effectively utilize both channel and

interference resources. Consequently, it demonstrates significant and consistent improvements in both the covert transmission rate and the transmission interruption probability, thereby providing an effective reference for the design of cooperative covert communication systems under partial CSI.

2. System Model and Transmission Scheme

The overall transmission process consists of two phases, as shown in Figure 1. During the first phase, Alice sends the covert message to the Relay. In the second phase, the Relay adopts the DF protocol to forward the decoded information to Bob. Meanwhile, the Jammer radiates jamming signals toward Willie, who monitors whether either Alice or the Relay is active. For the entire end-to-end path to remain covert, both transmission hops must evade Willie's detection. Since no direct link exists between Alice and Bob, the Relay is indispensable for information forwarding.

Assume the transmission occurs in a slotted framework, where each time slot comprises channel uses, and all nodes are perfectly synchronized [24–26]. The wireless channels follow a standard Rayleigh block-fading process: the channel coefficient stays fixed over each slot and changes independently from slot to slot, with all links being mutually uncorrelated. The channel gain from node i to node j is given by $h_{i,j}d_{i,j}^{-\alpha/2}$, where $h_{ij} \sim CN(0,1)$ represents the small-scale Rayleigh fading coefficient, d_{ij} denotes the distance between the nodes, and α is the path-loss exponent.

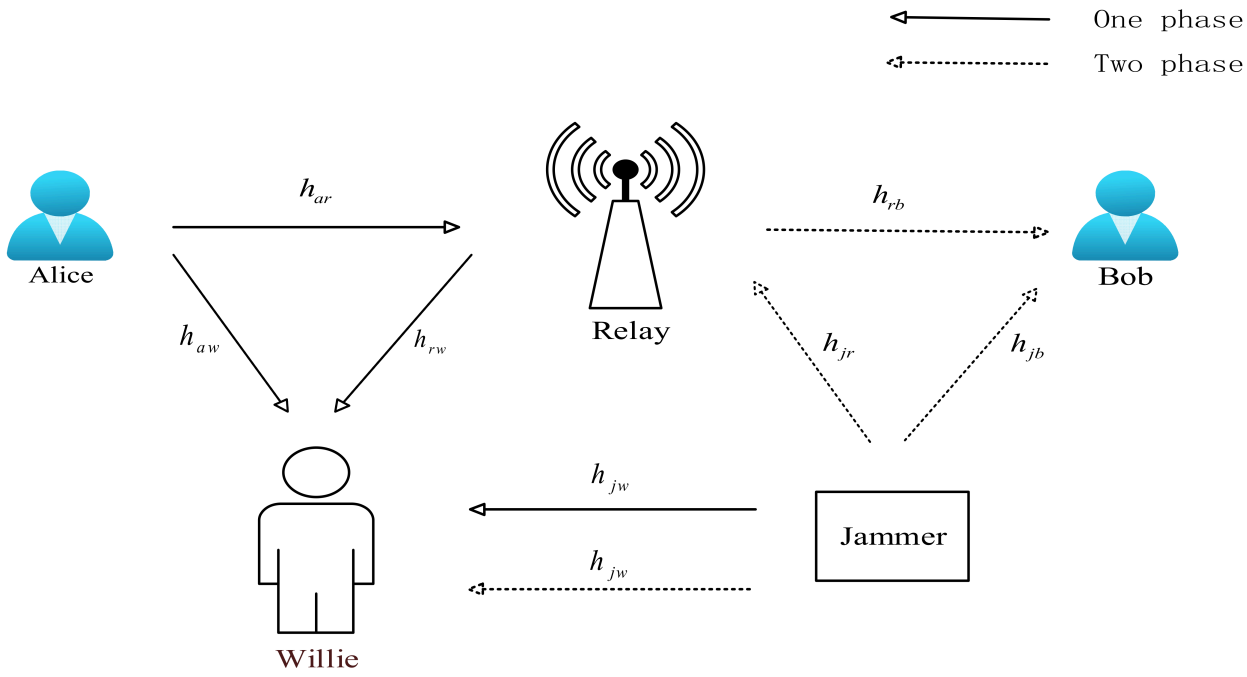


Figure 1. Cooperative covert communication system model assisted by a DF relay system.

It is assumed that the legitimate nodes have knowledge of the perfect CSI among themselves. Such an assumption, where cooperative nodes acquire signal prior information through shared parameters, is widely adopted in the literature [27,28]. However, they do not possess the CSI of the channels between themselves and the Jammer, nor between Willie and the Jammer. Willie knows the statistical CSI of the links to all legitimate nodes. The transmit power of the Jammer P_j is uniformly distributed over the interval, and Alice has this prior knowledge.

3. Phase One—Covert Message Transmission from Alice to the Relay

3.1. Relay Receiving the Covert Message

During the first phase, Alice delivers the covert message to the Relay while the Jammer radiates interfering signals toward Willie. The received signal at the Relay is written as

$$y_r[i] = \begin{cases} \sqrt{P_j} d_{jr}^{-\alpha/2} h_{jr} x_j[i] + n_r[i] & , H_0 \\ \sqrt{P_a} d_{ar}^{-\alpha/2} h_{ar} x_a[i] + \sqrt{P_j} d_{jr}^{-\alpha/2} h_{jr} x_j[i] + n_r[i] & , H_1 \end{cases} \tag{1}$$

where P_a and P_j denote the transmit powers of Alice and the Jammer, respectively. The covert signal $x_a[i]$ from Alice satisfies $[x_a[i]x_a^{\dagger}[i]] = 1, i = 1, 2, \cdots, N$. $x_j[i]$ is the jamming signal sent by the Jammer, satisfying $[x_j[i]x_j^{\dagger}[i]] = 1, i = 1, 2, \cdots, N$, and $n_r[i]$ is the additive white Gaussian noise (AWGN) at the Relay, i.e., $n_r[i] \sim CN(0, \sigma_r^2)$.

3.2. Control Strategy

In the first phase, according to Shannon's formula, when $C < R$, a transmission outage occurs, where $C = \log_2(1 + SINR_r)$, and $SINR_r = \frac{P_a d_{ar}^{-\alpha} |h_{ar}|^2}{P_j d_{jr}^{-\alpha} |h_{jr}|^2 + \sigma_r^2}$. When $C = R$, the minimum transmit power for Alice that guarantees no outage is given by

$$P_a^{\min} = \frac{2^R - 1}{d_{ar}^{-\alpha} |h_{ar}|^2} (P_j d_{jr}^{-\alpha} |h_{jr}|^2 + \sigma_r^2) \tag{2}$$

Proof. Substituting $C = \log_2(1 + SINR_r)$ into $C = R$, we have

$$\log_2(1 + SINR_r) = R \tag{3}$$

Finally, through straightforward mathematical manipulation, we arrive at Equation (2), namely

$$P_a^{\min} = \frac{2^R - 1}{d_{ar}^{-\alpha} |h_{ar}|^2} (P_j d_{jr}^{-\alpha} |h_{jr}|^2 + \sigma_r^2) \tag{4}$$

□

Since acquiring real-time CSI of the Alice–Jammer link is infeasible for Alice, we construct a one-sided confidence interval $[0, \lambda_1]$ using statistical knowledge, where λ_1 serves as the upper confidence bound for $|h_{jr}|^2$. The transmit power $P_a^{\min}$ can then be estimated as

$$P_a^{\min} = \frac{K_1}{|h_{ar}|^2} (P_j d_{jr}^{-\alpha} \lambda_1 + \sigma_r^2) \tag{5}$$

To simplify the notation, we define $K_1 \triangleq \frac{2^R - 1}{d_{ar}^{-\alpha}}$.

Based on Equation (5), we have

$$|h_{ar}|^2 = \frac{K_1}{P_a^{\min}} (P_j d_{jr}^{-\alpha} \lambda_1 + \sigma_r^2) \tag{6}$$

Since $P_a^{\min}$ approaches infinity when $|h_{ar}|^2$ is very small, a truncation point Q_1 is set as the lower bound of. As P_a increases, $|h_{ar}|^2$ decreases. When P_a reaches its maximum value $P_a^{\max}$, $|h_{ar}|^2$ attains its lower bound. The truncation point is then given by

$$Q_1 = \frac{K}{P_a^{\max}} (\frac{P_j^{\max}}{2} d_{jr}^{-\alpha} \lambda_1 + \sigma_r^2) \tag{7}$$

https://doi.org/10.3390/telecom7050126

According to Reference [11], the transmission strategy for Alice is as follows:

$$P_a = \left\{ \begin{array}{ll} \frac{K_1}{|h_{ar}|^2}(P_j d_{jr}^{-\alpha}\lambda_1 + \sigma_r^2), |h_{ar}|^2 \geq Q_1 \\ 0 \qquad\qquad\qquad , \quad else \end{array} \right\} \tag{8}$$

where $K_1 = \frac{2^R-1}{d_{ar}^{-\alpha}}$ and λ_1 provides the confidence upper bound for $|h_{jr}|^2$ as $[0, \lambda_1]$, and the transmission probability for Alice is

$$P_{G_1} = \Pr(|h_{ar}|^2 \geq Q_1) = e^{-Q_1} \tag{9}$$

Proof. Since $h_{ar} \sim CN(0,1)$, the probability density function (PDF) of $|h_{ar}|^2$ is $f_X(x) = e^{-x}$, $x \geq 0$. Therefore, the transmission probability for Alice is

$$\begin{array}{rcl} P_{G_1} & = & \Pr(|h_{ar}|^2 \geq Q_1) \\ & = & \int_{Q_1}^{\infty} e^{-x} dx \end{array} \tag{10}$$

Finally, Equation (9) can be obtained through straightforward mathematical operations. □

3.3. Analysis of Detection Metric and Performance

3.3.1. Analysis of the Detection Metric

Willie conducts a binary hypothesis test to decide whether active transmission exists. Specifically, H_0 denotes the null hypothesis that Alice remains silent, while H_1 corresponds to the alternative that either Alice or the Relay is engaged in covert transmission.

In the first phase, the received signal at Willie is given by

$$y_w^1[i] = \left\{ \begin{array}{l} \sqrt{P_j} h_{jw} d_{jw}^{-\alpha/2} x_j[i] + n_w[i] \qquad\qquad , H_0 \\ \sqrt{P_a} h_{aw} d_{aw}^{-\alpha/2} x_a[i] + \sqrt{P_j} h_{jw} d_{jw}^{-\alpha/2} x_j[i] + n_w[i], H_1 \end{array} \right. \tag{11}$$

where $x_a[i]$ denotes the covert signal from Alice with unit power, i.e., $[x_a[i] x_a^{\dagger}[i]] = 1$, $i = 1, 2, \cdots, N$, and $n_w[i]$ is the AWGN distributed as $n_w[i] \sim CN(0, \sigma_w^2)$.

Within one communication time slot, to minimize the detection error probability, Willie adopts a likelihood ratio test, formulated as

$$\frac{p_1(y_w)}{p_0(y_w)} \underset{D_0}{\overset{D_1}{\gtrless}} 1 \tag{12}$$

where $p_1(y_w)$ and $p_0(y_w)$ are the PDF under hypothesis H_1 and H_0, respectively. D_1 and D_0 represent Willie's decision that Alice is transmitting a signal and is not transmitting a signal, respectively.

With equal prior probabilities, Willie's detection error probability is $\xi_1 \triangleq P_{FA}^1 + P_{MD}^1$, with $P_{FA}^1 = \Pr\{D_1|H_0\}$ and $P_{MD}^1 = \Pr\{D_0|H_1\}$. The detection error rate in the first phase can be expressed as

$$\xi_1 = P_{FA}^1 + P_{MD}^1 \tag{13}$$

3.3.2. Analysis of Detection Performance

In covert communication scenarios, the covertness constraint is typically expressed as $\xi > 1 - \varepsilon$, where $\varepsilon > 0$ can be arbitrarily small. The minimum error detection rate is determined by the total variation distance $V_T(p_1|p_0)$ between $p_1(y_w)$ and $p_0(y_w)$ as

$$\xi_1^* = 1 - V_T(P_{H_1}|P_{H_0}) \tag{14}$$

According to Pinsker's inequality, the relative entropy upper bound for the total variation distance between is given by

$$V_T(P_{H_1}|P_{H_0}) \leq \sqrt{\frac{1}{2}D(P_{H_1}\|P_{H_0})} \tag{15}$$

Thus, a stricter average covertness constraint for the first phase can be expressed as

$$\frac{P_a d_{aw}^{-\alpha}}{P_j^{\max} d_{jw}^{-\alpha} + \sigma_w^2} \leq \varepsilon \tag{16}$$

Proof. The minimum error detection rate is lower-bounded as

$$\xi_1^* \geq 1 - \sqrt{\frac{1}{2}D(P_{H_1}\|P_{H_0})} \tag{17}$$

When $\sqrt{\frac{1}{2}D(P_{H_1}\|P_{H_0})} \leq \varepsilon$, the requirement $\xi \geq 1-\varepsilon$ is fully satisfied. Thus, the covertness constraint for the first phase can be written as

$$\sqrt{\frac{1}{2}D(P_{H_1}\|P_{H_0})} \leq \varepsilon \tag{18}$$

For complex Gaussian distributions, according to Reference [27], $D(P_{H_1}\|P_{H_0})$ is calculated as

$$\begin{aligned} D(P_{H_1}\|P_{H_0}) &= \int_{-\infty}^{\infty} f_{H_1}(y_w^1) \ln \frac{f_{H_1}(y_w^1)}{f_{H_0}(y_w^1)} dy_w^1 \\ &= N(\gamma_w^1 - \ln(1+\gamma_w^1)) \end{aligned} \tag{19}$$

where $\gamma_w^1 = \frac{P_a d_{aw}^{-\alpha}|h_{aw}|^2}{P_j d_{aw}^{-\alpha}|h_{jw}|^2 + \sigma_w^2}$ and is the number of channel uses per time slot.

Since Alice only knows the statistical CSI and, she replaces the KL divergence with the average KL divergence as the covertness constraint:

$$E\{\sqrt{\frac{1}{2}D_1(P_{H_1}^1\|P_{H_0}^1)}\} = E\{\sqrt{\frac{\gamma_w^1 - \ln(1+\gamma_w^1)}{2}}\} \leq \varepsilon \tag{20}$$

Following the approach in [29], in covert communications, is typically a very small value. When $x \to 0$, we have $x - \ln(1+x) \approx \frac{1}{2}x^2$, and $D(P_{H_0}|P_{H_1}) = \gamma_w - \ln(1+\gamma_w) \approx \frac{1}{2}\gamma_W^2$. Substituting the approximated KL divergence into the average covertness constraint yields

$$E\{\sqrt{\frac{1}{2}D_1(P_{H_1}^1\|P_{H_0}^1)}\} \approx \frac{1}{2}E\{\gamma_w\} \tag{21}$$

Substituting into Equation (18) gives

$$E\{\sqrt{\frac{1}{2}D_1(P_{H_1}^1\|P_{H_0}^1)}\} \approx \frac{1}{2}E\{\gamma_w\} = \frac{1}{2}\frac{P_a d_{aw}^{-\alpha}}{P_j d_{aw}^{-\alpha} + \sigma_w^2} \leq \varepsilon \tag{22}$$

Finally, the average covertness constraint is obtained as

$$\frac{P_a d_{aw}^{-\alpha}}{P_j^{\max} d_{jw}^{-\alpha} + \sigma_w^2} \leq \varepsilon \tag{23}$$

The average covert constraint can characterize the average covert performance, but it fails to guarantee covertness in every time slot. □

When Alice transmits information using Equation (8), the closed-form covertness constraint for the first phase is obtained as

$$\lambda_1 \leq \frac{2}{P_j^{\max}}\left(\frac{A_1 d_{jr}^{\alpha}}{K} - d_{jr}^{\alpha}\sigma_r^2\right) \tag{24}$$

where $A_1 = \varepsilon d_{aw}^{\alpha}\left(\frac{P_j^{\max} d_{jw}^{-\alpha}}{2} + \sigma_w^2\right)$.

Proof. Substituting Equation (8) into Equation (23), we have

$$P_a \leq \varepsilon d_{aw}^{\alpha}\left(\frac{P_j^{\max} d_{jw}^{-\alpha}}{2} + \sigma_w^2\right) \tag{25}$$

Let $\varepsilon d_{aw}^{\alpha}\left(\frac{P_j^{\max} d_{jw}^{-\alpha}}{2} + \sigma_w^2\right) = A_1$; substituting Equation (8) and performing simple mathematical operations, we have

$$\lambda_1 \leq \frac{A|h_{ar}|^2}{K_1 d_{jr}^{-\alpha} P_j} - \frac{\sigma_r^2}{d_{jr}^{-\alpha} P_j} \tag{26}$$

Since P_j and $|h_{ar}|^2$ are random variables, this paper derives the closed-form expression of the confidence interval using the average expectation. Where $P_j \sim U(0, P_j^{\max})$ and $h_{ar} \sim CN(0,1)$, we have

$$\lambda_1 \leq E\left[\frac{A|h_{ar}|^2}{K_1 d_{jr}^{-\alpha} P_j} - \frac{\sigma_r^2}{d_{jr}^{-\alpha} P_j}\right] \tag{27}$$

Finally, through simple mathematical operations, we can obtain Equation (24), namely

$$\lambda_1 \leq \frac{2}{P_j^{\max}}\left(\frac{A d_{jr}^{\alpha}}{K} - d_{jr}^{\alpha}\sigma_r^2\right) \tag{28}$$

□

3.4. Analysis of Covert Performance

3.4.1. Analysis of Transmission Outage Probability

With Alice's power policy in (8), the received SINR at the Relay is

$$SINR_r = (2^R - 1)\frac{\left(P_j d_{ar}^{-\alpha}\lambda_1 + \sigma_r^2\right)}{P_j d_{jr}^{-\alpha}|h_{jr}|^2 + \sigma_r^2} \tag{29}$$

Proof.

$$SINR_r = \frac{P_a d_{ar}^{-\alpha}|h_{ar}|^2}{P_j d_{jr}^{-\alpha}|h_{jr}|^2 + \sigma_r^2} \tag{30}$$

By substituting Equation (8), we have

$$SINR_r = (2^R - 1)\frac{\left(P_j d_{jr}^{-\alpha}\lambda_1 + \sigma_r^2\right)}{P_j d_{jr}^{-\alpha}|h_{jr}|^2 + \sigma_r^2} \tag{31}$$

Since $C = \log_2(1 + SINR_r)$, an outage occurs when $C < R$; therefore, the transmission outage probability is

$$\delta_1 = e^{-\lambda_1} \tag{32}$$

□

Proof. When $C < R$, the transmission outage probability can be expressed as

$$\delta_1 = \Pr(C < R) \tag{33}$$

By substituting Equation (31), we have

$$(2^R - 1)\frac{(P_j d_{ar}^{-\alpha}\lambda_1 + \sigma_r^2)}{P_j d_{jr}^{-\alpha}|h_{jr}|^2 + \sigma_r^2} < (2^R - 1) \tag{34}$$

Since $h_{jr} \sim CN(0,1)$, the PDF of $|h_{jr}|^2$ is $f_X(x) = e^{-x},\ x \geq 0$. Substituting the PDF of $|h_{jr}|^2$ into the expression and performing some straightforward mathematical manipulations, we arrive at Equation (31), namely

$$\delta_1 = e^{-\lambda_1} \tag{35}$$

□

3.4.2. Analysis of Covert Transmission Rate

From Equations (9) and (35), the effective transmission rate in the first phase is given by

$$\eta_1 = R(1 - \delta_1)P_{G_1} \tag{36}$$

From Equations (28) and (36), the maximum covert rate for the first phase is given by

$$\begin{aligned} &\max_{\lambda_1} \quad \eta_1 \\ &s.t. \quad \lambda_1 \leq \tfrac{2}{P_j^{\max}}\left(\tfrac{A_1 d_{jr}^{\alpha}}{K} - d_{jr}^{\alpha}\sigma_r^2\right) \end{aligned} \tag{37}$$

4. Second Phase—Covert Message Transmission from Relay to Receiver

This section first presents the received signal at Bob in the second phase. Based on this, an adaptive transmit power strategy for the Relay is derived. Subsequently, Willie's detection metric and performance are analyzed, leading to the derivation of the transmission outage probability and the effective transmission rate for this phase. Finally, the objective function for the second phase is formulated.

4.1. Covert Information Reception at the Receiver

In the second phase, after decoding the signal from Alice, the relay forwards it to Bob. The transmitted signal at the relay is

$$x_r[i] = \hat{x}_a[i] \tag{38}$$

$\hat{x}_a[i]$ denotes the decoded and re-encoded information recovered at the relay from the received signal. Meanwhile, the Jammer transmits an interference signal to Willie. Accordingly, the signal received at Bob is given by

$$y_b[i] = \begin{cases} \sqrt{P_j} d_{jb}^{-\alpha/2} h_{jb} x_j[i] + n_b[i] & , H_0 \\ \sqrt{P_r} d_{rb}^{-\alpha/2} h_{rb} x_r[i] + \sqrt{P_j} d_{jb}^{-\alpha/2} h_{jb} x_j[i] + n_b[i] & , H_1 \end{cases} \tag{39}$$

where P_r and P_j are the transmit power of the Relay and the Jammer, respectively. $x_j[i]$ is the jamming signal transmitted by the Jammer with $[x_r[i]x_r^{\dagger}[i]] = 1, i = 1, 2, \cdots, N$. And $n_b[i]$ is AWGN at Bob, given by $n_b[i] \sim CN(0, \sigma_b^2)$.

4.2. Control Strategy

In a manner similar to the first phase, we substitute $C = \log_2(1 + SINR_r)$ into $C = R$ to obtain $P_r^{\min}$. Following this, the truncation point is calculated using an approach analogous to that in Equation (6). Accordingly, the transmission strategy of the Relay is defined as

$$P_r = \begin{cases} \frac{K_2}{|h_{rb}|^2}(P_j d_{jb}^{-\alpha}\lambda_2 + \sigma_b^2), |h_{rb}|^2 \geq Q_2 \\ 0 \qquad\qquad\qquad , \quad else \end{cases} \tag{40}$$

where $K_2 = \frac{2^R - 1}{d_{rb}^{-\alpha}}$, $Q_2 = \frac{K}{P_r^{\max}}(\frac{P_j^{\max}}{2} d_{jr}^{-\alpha}\lambda_2 + \sigma_b^2)$.
Therefore, the transmission probability of the Relay is given by

$$P_{G_1} = \Pr(|h_{rb}|^2 \geq Q_2) = e^{-Q_2} \tag{41}$$

4.3. Analysis of Detection Metric and Performance

4.3.1. Analysis of the Detection Metric

Willie's detection objective shifts to determining whether the Relay is forwarding information. The binary hypothesis test is formulated as follows: H_0, the Relay is not transmitting, and H_1, the Relay is forwarding a covert signal. Accordingly, the signal received by Willie is given by

$$y_w^2[i] = \begin{cases} \sqrt{P_j} h_{jw} d_{jw}^{-\alpha/2} x_j[i] + n_w[i] & , H_0 \\ \sqrt{P_r} h_{rw} d_{rw}^{-\alpha/2} x_r[i] + \sqrt{P_j} h_{jw} d_{jw}^{-\alpha/2} x_j[i] + n_w[i], & H_1 \end{cases} \tag{42}$$

Within one communication time slot, Willie must make a decision to determine whether the Relay is transmitting. Willie adopts a likelihood ratio test to minimize his detection error probability:

$$\frac{p_1(y_w)}{p_0(y_w)} \underset{D_0}{\overset{D_1}{\gtrless}} 1 \tag{43}$$

where $p_1(y_w)$ and $p_0(y_w)$ are the PDF of y_w under hypotheses H_1 and H_0, respectively; and D_1 and D_0 represent Willie's decision that Alice is transmitting and not transmitting, respectively.
Considering equal prior probabilities, Willie's detection error rate can be defined as $\xi_2 \triangleq P_{FA}^2 + P_{MD}^2$, where $P_{FA}^2 = \Pr\{D_1|H_0\}$ and $P_{MD}^2 = \Pr\{D_0|H_1\}$. Consequently, the detection error rate in the second phase can be expressed as

$$\xi_2 = P_{FA}^2 + P_{MD}^2 \tag{44}$$

4.3.2. Analysis of Detection Performance

Adopting the same analytical approach as in the first phase, the expression for the average covertness constraint in the second phase is obtained as

$$\frac{P_r d_{rw}^{-\alpha}}{P_j d_{rw}^{-\alpha} + \sigma_w^2} \leq \varepsilon \tag{45}$$

Similarly, the covertness constraint for the second phase is given by

$$\lambda_2 \leq \frac{2}{P_j^{\max}}(\frac{A_2 d_{jb}^{\alpha}}{K} - d_{jb}^{\alpha}\sigma_b^2) \tag{46}$$

where $A_2 = \varepsilon d_{rw}^{\alpha}(\frac{P_j^{\max} d_{jw}^{-\alpha}}{2} + \sigma_w^2)$.

4.4. Analysis of Covert Performance

4.4.1. Analysis of Transmission Outage Probability

Following the same principle as in the first phase, the relay adopts the power policy in (40). The received SINR at Bob is

$$SINR_b = (2^R - 1)\frac{(P_j d_{jb}^{-\alpha}\lambda_2 + \sigma_b^2)}{P_j d_{jb}^{-\alpha}|h_{jb}|^2 + \sigma_b^2} \tag{47}$$

Similar to the first phase and based on $C = \log_2(1 + SINR_b)$, transmission outage is declared if $C < R$; the outage probability can be expressed as

$$\delta_2 = e^{-\lambda_2} \tag{48}$$

4.4.2. Analysis of Covert Transmission Rate

From Equations (41) and (48), the effective transmission rate in the second phase is given by

$$\eta_2 = R(1 - \delta_2)P_{G_2} \tag{49}$$

Combining Equations (46) and (49), the maximum effective covert rate in the second phase is obtained as

$$\begin{aligned} &\max_{\lambda_2} \quad \eta_2 \\ &s.t. \quad \lambda_2 \le \tfrac{2}{P_j^{\max}}\left(\tfrac{A_2 d_{jb}^{\alpha}}{K} - d_{jb}^{\alpha}\sigma_b^2\right) \end{aligned} \tag{50}$$

5. Analysis of Overall Covert Performance

This section first presents the overall system transmission outage probability, followed by the overall system covert transmission rate.

5.1. Analysis of Overall System Transmission Outage Probability

Denoting the transmission outage probability in the first phase as δ_1 and that in the second phase as δ_2, the overall transmission outage probability is therefore given by

$$\delta = 1 - (1 - \delta_1)(1 - \delta_2) \tag{51}$$

By substituting the transmission outage probability expressions for the two phases from Equations (35) and (48) into Equation (51), the overall transmission outage probability is consequently given by

$$\delta = 1 - (1 - e^{-\lambda_1})(1 - e^{-\lambda_2}) \tag{52}$$

5.2. Analysis of Overall System Covert Transmission Rate

For the DF relay-assisted cooperative covert communication system, unlike the overall transmission outage probability, determining the overall maximum effective covert rate requires the consideration of the maximum effective covert rates in both phases. Specifically, it is defined as the minimum of the maximum effective covert rates from the two phases:

$$\begin{aligned} &\eta = min\{\eta_1, \eta_2\} \\ &s.t. \quad \lambda_1 \le \tfrac{2}{P_j^{\max}}\left(\tfrac{A_1 d_{jr}^{\alpha}}{K} - d_{jr}^{\alpha}\sigma_r^2\right) \\ &\qquad \lambda_2 \le \tfrac{2}{P_j^{\max}}\left(\tfrac{A_2 d_{jb}^{\alpha}}{K} - d_{jb}^{\alpha}\sigma_b^2\right) \end{aligned} \tag{53}$$

6. Numerical Results

The covert performance of the proposed scheme is evaluated via simulations in the DF relay and jammer-aided cooperative covert system. A comparison is made against a constant-power baseline, where the transmit power is optimized to maximize the covert throughput. The distances between the nodes [11] are $d_{ar} = d_{rb} = 400$ m, $d_{aw} = d_{jw} = d_{jr} = d_{jb} = 1000$ m, and $\sigma_w^2 = \sigma_r^2 = \sigma_b^2 = -120$ dBm.

Figure 2 illustrates the relationship between the covertness constraint value ε and the total covert transmission rate η under different transmission strategies at the maximum jamming power. The results demonstrate that the adaptive power strategy achieves a superior total covert rate compared to the constant power strategy in DF cooperative covert communication. When the covertness constraint ε is very stringent, the adaptive strategy ensures that the condition $C = R$ is satisfied over most channel realizations by operating at the minimum transmit power P_a required to avoid transmission outage. This results in a marginally higher covert rate. As ε increases, the covert rate η of the adaptive strategy surpasses that of the constant power strategy rapidly. This performance gain is attributed to the ability of the adaptive strategy to dynamically adjust the confidence interval $\lambda_{1(2)}$, thereby minimizing the transmission outage probability. This advantage becomes more pronounced at higher target transmission rates R. In conclusion, as inferred from the preceding analysis, the adaptive power strategy significantly enhances the covert transmission rate under relatively relaxed covertness constraints.

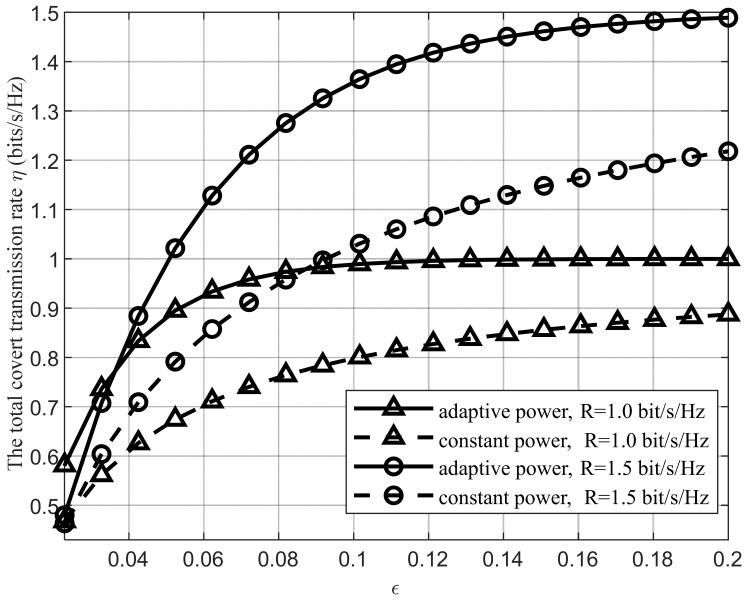


Figure 2. The relationship between parameter ε and the total covert transmission rate η under different transmission strategies in condition $P_j^{\max} = 10$ dBm.

Figure 3 depicts the relationship between the transmission rate R and the optimized upper confidence bound λ_1 in the first phase under different maximum jamming power levels $P_j^{\max}$. As observed from Figure 3, the confidence bound λ_1 is a decreasing function of the transmission rate R. Furthermore, the upper limit of this confidence bound is jointly determined by both R and $P_j^{\max}$. This behavior occurs because a higher target transmission rate necessitates a reduction in power allocation to satisfy the stringent covertness constraints. Additionally, a larger $P_j^{\max}$ corresponds to a higher λ_1 This is because, under elevated jamming power, the adaptive power strategy can afford to increase λ_1 to maximize the covert transmission rate without violating the covertness requirements.

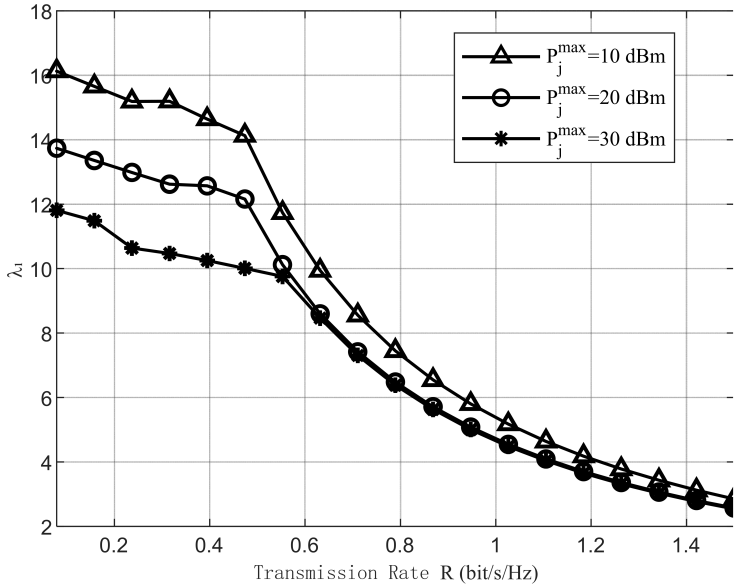


Figure 3. The transmission rate R and the optimized upper confidence bound λ_1 as a function of the maximum jamming power $P_j^{\max}$ under a covertness constraint of $\varepsilon = 0.1$.

Figure 4 shows the relationship between the covertness constraint and the total transmission outage probability δ for different transmission strategies when $P_j^{\max} = 10$ dBm. As the covertness constraint ε is relaxed, the system's total transmission outage probability decreases significantly. For any given value of ε, the outage probability of the adaptive power strategy is consistently lower than that of the constant power strategy. Furthermore, a higher transmission rate R leads to an overall increase in the outage probability because it requires a higher signal-to-interference-plus-noise ratio (SINR) threshold. In conclusion, the adaptive power strategy enhances the reliability of the DF relay-assisted cooperative covert communication system. This improvement is more pronounced under looser covertness constraints.

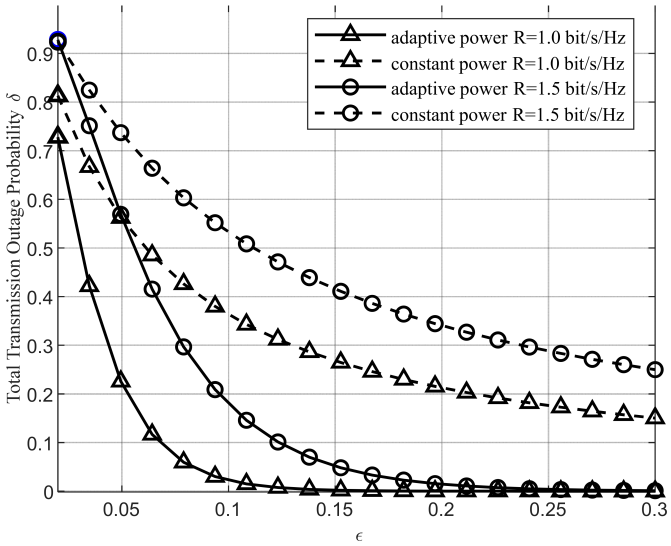


Figure 4. The relationship between and the total transmission outage probability δ under different transmission strategies when $P_j^{\max} = 10$ dBm.

Figure 5 illustrates the total transmission outage probability versus the maximum jamming power $P_j^{\max}$ for two target rates, $R = 1$ and $R = 1.5$ bpcu, comparing both adaptive and constant power strategies. The results demonstrate that the adaptive power strategy consistently achieves a lower outage probability than the constant-power baseline

across all jamming power levels. For $R = 1.5$ bpcu, the outage probability is higher than for $R = 1$ bpcu in both strategies, as a higher target rate requires a higher SINR threshold. Moreover, as $P_j^{\max}$ increases, the outage probability decreases for both strategies, because the increased jamming power relaxes the covertness constraint and allows higher transmit power. However, the adaptive strategy exhibits a more rapid decrease, confirming its superior ability to exploit the available interference uncertainty for reliability enhancement.

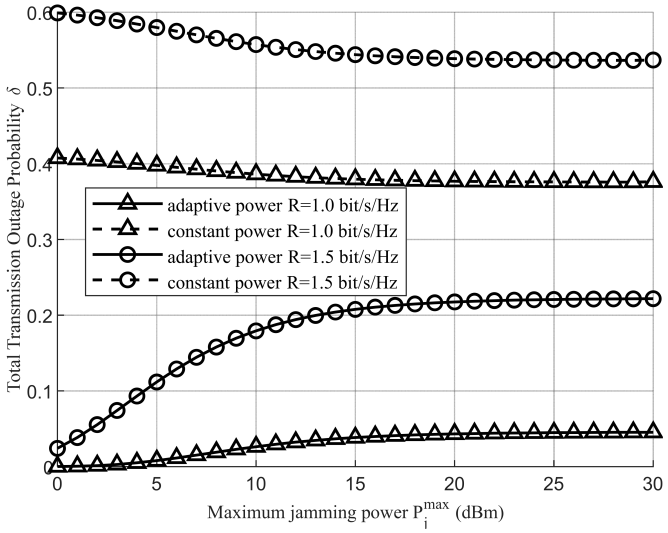


Figure 5. Total transmission outage probability versus maximum jamming power $P_j^{\max}$ for different target transmission rates R.

Figure 6 shows the total covert transmission rate versus $P_j^{\max}$ for $R = 1$ and $R = 1.5$ bpcu. The adaptive power strategy significantly outperforms the constant-power strategy, especially for higher target rates. For $R = 1.5$ bpcu, the performance gap between the two strategies is more pronounced, as the adaptive scheme dynamically adjusts the transmit power to meet the higher rate requirement while maintaining covertness. As $P_j^{\max}$ increases, the covert transmission rate increases for both strategies, due to the relaxed covertness constraint and the corresponding increase in allowable transmit power. These results collectively validate that the proposed adaptive power control strategy effectively balances the trade-off between covertness and transmission reliability.

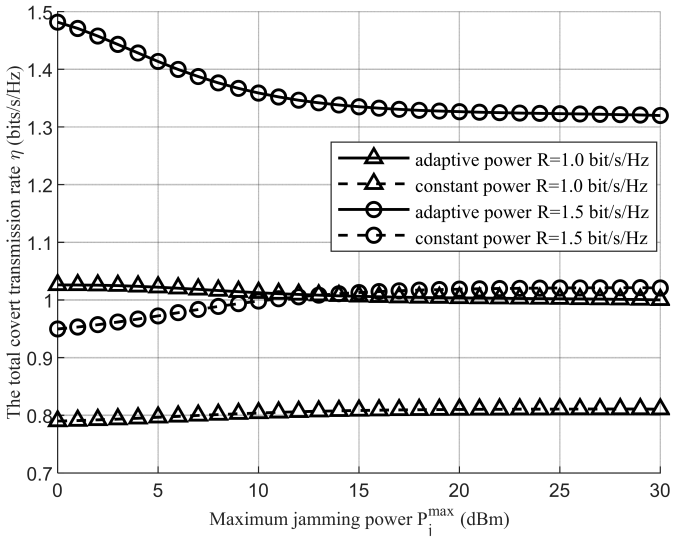


Figure 6. Total covert transmission rate versus maximum jamming power $P_j^{\max}$ for different target transmission rates R.

7. Conclusions

This paper addresses the cooperative covert communication system employing a DF relay with CSI and proposes an adaptive power control scheme. The proposed scheme constructs confidence intervals to estimate the unknown channel parameters. By dynamically adjusting the transmit power based on these estimates, it effectively reduces the system outage probability while satisfying the KL divergence-based covertness constraint. The numerical results demonstrate that the adaptive power strategy significantly enhances the system's covert transmission rate compared to the constant power strategy. This performance improvement is particularly pronounced under relatively relaxed covertness constraints. Furthermore, the proposed strategy also markedly reduces the system's transmission outage probability. These findings collectively validate the superiority of the proposed strategy in effectively balancing the fundamental trade-off between covertness and reliability.

Author Contributions: Conceptualization, L.Y. and L.T.; methodology, W.L.; software, W.L. and Y.T.; validation, Z.H., J.H. and Y.L.; formal analysis, W.L. and Z.S.; investigation, W.L.; resources, L.Y. and L.T.; data curation, W.L.; writing—original draft preparation, W.L.; writing—review and editing, L.Y. and L.T.; visualization, Y.T.; supervision, L.Y. and L.T.; project administration, L.Y.; funding acquisition, L.Y. All authors have read and agreed to the published version of the manuscript.

Funding: This work was supported by the National Natural Science Foundation of China (Grant No. 62303177), the Natural Science Foundation of Hunan Province (Grant No. 2021JJ50051), and the Natural Science Foundation of Hunan Province (Grant No. 2024JJ6209).

Institutional Review Board Statement: Not applicable.

Informed Consent Statement: Not applicable.

Data Availability Statement: The original contributions presented in this study are included in the article. Further inquiries can be directed to the corresponding author.

Conflicts of Interest: The authors declare no conflicts of interest.

References

1. Tang, R.; Yang, L.; Lv, L.; Zhang, Z.; Liu, Y.; Chen, J. Dual-Functional Artificial Noise (DFAN) Aided Robust Covert Communications in Integrated Sensing and Communications. *IEEE Trans. Commun.* **2025**, *73*, 1072–1086. [CrossRef]
2. Yang, G.; Qian, Y.; Ren, K.; Mei, Z.; Shu, F.; Zhou, X.; Wu, W. Covert Wireless Communications for Augmented Reality Systems with Dual Cooperative UAVs. *IEEE J. Sel. Top. Signal Process.* **2023**, *17*, 1119–1130. [CrossRef]
3. Gao, C.; Yang, B.; Jiang, X.; Inamura, H.; Fukushi, M. Covert Communication in Relay-Assisted IoT Systems. *IEEE Internet Things J.* **2021**, *8*, 6313–6323. [CrossRef]
4. Wang, X.; Du, H.; Gao, Y.; Zhang, J.; Niyato, D.; Letaief, K.B. Secure Body-Centric Internet of Things Networks: Physical Layer Security versus Covert Communication. *IEEE Trans. Wirel. Commun.* **2024**, *23*, 12731–12748. [CrossRef]
5. Du, J.; Tian, W.; Ji, X.; Du, M.; Liu, G.; Dai, Y.; Han, Z. Strategic UAV-Assisted Game Model for Detection in Covert Communication. *IEEE Trans. Veh. Technol.* **2023**, *72*, 7426–7438. [CrossRef]
6. Ma, Y.; Ma, R.; Yang, W.; Miao, C.; Cai, Y.; Wu, W. Covert Communication Using Time Modulated Retrodirective Array. *IEEE Wirel. Commun. Lett.* **2024**, *13*, 510–514. [CrossRef]
7. Zhang, Y.; Ni, W.; Mao, Y.; Ning, B.; Xiao, S.; Tang, W.; Niyato, D. Rate-Splitting Multiple Access for Covert Communications. *IEEE Wirel. Commun. Lett.* **2024**, *13*, 1685–1689. [CrossRef]
8. Thanh Hai, N.; Le Khoa, D. Preserving Covert Communication in Downlink NOMA Systems via Reradiating on Antennas. *IEEE Commun. Lett.* **2023**, *27*, 3098–3102. [CrossRef]
9. Su, Y.; Fu, S.; Si, J.; Xiang, C.; Zhang, N. Optimal Hovering Height and Power Allocation for UAV-Aided NOMA Covert Communication System. *IEEE Wirel. Commun. Lett.* **2023**, *12*, 937–941. [CrossRef]
10. Hadzi-Velkov, Z.; Pejoski, S.; Zlatanov, N. Achieving Near Ideal Covertness in NOMA Systems with Channel Inversion Power Control. *IEEE Commun. Lett.* **2022**, *26*, 2542–2546. [CrossRef]
11. He, R.; Li, G.; Wang, H.; Jiao, Y.; Cai, J. Adaptive Power Control for Cooperative Covert Communication with Partial Channel State Information. *IEEE Wirel. Commun. Lett.* **2022**, *11*, 1428–1432. [CrossRef]

12. He, R.; Li, G.; Wang, H.; Jiao, Y.; Cai, J. Channel-Aware Jammer Selection and Power Control in Covert Communication. *IEEE Trans. Veh. Technol.* **2024**, *73*, 2266–2279. [CrossRef]
13. Ma, R.; Yang, X.; Pan, G.; Guan, X.; Zhang, Y.; Yang, W. Covert Communications with Channel Inversion Power Control in the Finite Blocklength Regime. *IEEE Wirel. Commun. Lett.* **2021**, *10*, 835–839. [CrossRef]
14. Sun, R.; Wu, H.; Yang, B.; Shen, Y.; Yang, W.; Jiang, X.; Taleb, T. On Covert Rate in Full-Duplex D2D-Enabled Cellular Networks with Spectrum Sharing and Power Control. *IEEE Trans. Mob. Comput.* **2024**, *23*, 9931–9945. [CrossRef]
15. Sun, R.; Yang, B.; Ma, S.; Shen, Y.; Jiang, X. Covert Rate Maximization in Wireless Full-Duplex Relaying Systems with Power Control. *IEEE Trans. Commun.* **2021**, *69*, 6198–6212. [CrossRef]
16. Wang, M.; Yang, W.; Lu, X.; Hu, C.; Liu, B.; Lv, X. Channel Inversion Power Control Aided Covert Communications in Uplink NOMA Systems. *IEEE Wirel. Commun. Lett.* **2022**, *11*, 871–875. [CrossRef]
17. Mu, P.; Li, Z.; Wang, B. Secure On–Off Transmission in Slow Fading Wiretap Channel with Imperfect CSI. *IEEE Trans. Veh. Technol.* **2017**, *66*, 9582–9586. [CrossRef]
18. Hashida, H.; Kawamoto, Y.; Kato, N. Selective Reflection Control: Distributed IRS-Aided Communication with Partial Channel State Information. *IEEE Trans. Veh. Technol.* **2022**, *71*, 11949–11958. [CrossRef]
19. Xu, H.; Ouyang, C.; Yang, H. RIS-Assisted mmWave MIMO Communications with Finite-Alphabet Inputs and Partial CSI. *IEEE Wirel. Commun. Lett.* **2024**, *13*, 1339–1343. [CrossRef]
20. Wang, M.; Xu, Z.; Xia, B.; Guo, Y.; Chen, Z. DF Relay Assisted Covert Communications: Analysis and Optimization. *IEEE Trans. Veh. Technol.* **2023**, *72*, 4073–4078. [CrossRef]
21. Lin, M.; Liu, C.; Wu, Q.; Wang, W. DF-Relay-Assisted Multiantenna D2D Covert Communication in the Presence of Joint Detection. *IEEE Internet Things J.* **2024**, *11*, 11800–11811. [CrossRef]
22. Lin, M.; Liu, C.; Wang, W. Relay-Assisted Uplink Covert Communication in the Presence of Multi-Antenna Warden and Uninformed Jamming. *IEEE Trans. Commun.* **2024**, *72*, 2124–2137. [CrossRef]
23. Bash, B.A.; Goeckel, D.; Towsley, D. Limits of Reliable Communication with Low Probability of Detection on AWGN Channels. *IEEE J. Sel. Areas Commun.* **2013**, *31*, 1921–1930. [CrossRef]
24. Shahzad, K.; Zhou, X.; Yan, S.; Hu, J.; Shu, F.; Li, J. Achieving Covert Wireless Communications Using a Full-Duplex Receiver. *IEEE Trans. Wirel. Commun.* **2018**, *17*, 8517–8530. [CrossRef]
25. Sobers, T.V.; Bash, B.A.; Guha, S.; Towsley, D.; Goeckel, D. Covert Communication in the Presence of an Uninformed Jammer. *IEEE Trans. Wirel. Commun.* **2017**, *16*, 6193–6206. [CrossRef]
26. Ding, Z.; Leung, K.K.; Goeckel, D.L.; Towsley, D. Opportunistic Relaying for Secrecy Communications: Cooperative Jamming vs. Relay Chatting. *IEEE Trans. Wirel. Commun.* **2011**, *10*, 1725–1729. [CrossRef]
27. Chen, R.; Li, Z.; Shi, J.; Yang, L.; Hu, J. Achieving Covert Communication in Overlay Cognitive Radio Networks. *IEEE Trans. Veh. Technol.* **2020**, *69*, 15113–15126. [CrossRef]
28. He, R.; Li, G.; Chen, J.; Wang, H.; Guan, X.; Xu, Y.; He, W.; Xu, Y. Joint Power and Beamformer Optimization in Multi-Antenna Relay Covert System: Exploiting Public Users as Shelter. *IEEE Trans. Wirel. Commun.* **2025**, *24*, 385–400. [CrossRef]
29. Che, B.; Shi, H.; Yang, W.; Guan, X.; Ma, R. Covert Wireless Communication Against Jamming-Assisted Proactive Detection. *IEEE Wirel. Commun. Lett.* **2023**, *12*, 1304–1308. [CrossRef]

Disclaimer/Publisher's Note: The statements, opinions and data contained in all publications are solely those of the individual author(s) and contributor(s) and not of MDPI and/or the editor(s). MDPI and/or the editor(s) disclaim responsibility for any injury to people or property resulting from any ideas, methods, instructions or products referred to in the content.